Available online at www.sciencedirect.com
SciVerse ScienceDirect
Ceramics International 39 (2013) 7703–7708
CERAMICS INTERNATIONAL
www.elsevier.com/locate/ceramint

Internal bias field relaxation in poled Mn-doped $Pb(Mn_{1/3}Sb_{2/3})O_3$–Pb $(Zr,Ti)O_3$ ceramics

Gang Du, Ruihong Liang, Li Wang, Kui Li, Wenbin Zhang, Genshui Wang, Xianlin Dong*

Key Laboratory of Inorganic Functional Materials and Devices, Shanghai Institute of Ceramics, Chinese Academy of Sciences, 201800 Shanghai, China

Received 25 January 2013; received in revised form 27 February 2013; accepted 10 March 2013
Available online 16 March 2013

Abstract

The frequency, electric field cycling and temperature dependences of the polarization–electric field (*P–E*), strain–electric field (*S–E*) loops in poled Mn-doped $0.05Pb(Mn_{1/3}Sb_{2/3})O_3$–$0.50PbZrO_3$–$0.45PbTiO_3$ ceramics have been investigated. The *P–E* and *S–E* loops are strongly asymmetric corresponding to the presence of an internal bias field E_i after poling and aging, indicating that the domain walls are strongly pinned by preferentially oriented defect dipoles formed by the acceptor dopant ions (Mn^{2+}/Mn^{3+}) and O^{2-} vacancies. Whereas, the loops exhibit a tendency of changing from asymmetric shapes to normal symmetric ones with increasing electric field amplitude or decreasing frequency. Repeated electric field cycling as well as high temperature results in a similar effect. Meanwhile, the E_i reduces consequently, providing evidence of domain depinning or internal bias field relaxation. It is suggested that the reorientation of the defect dipoles and depinning of domain walls arising from high temperature or electric field cycling are responsible for this extrinsic internal bias field relaxation process.

Keywords: Piezoelectric ceramics; Internal bias field; Defect dipoles; Domain wall motion

1. Introduction

$Pb(Mn_{1/3}Sb_{2/3})O_3$–$Pb(Zr,Ti)O_3$ (PMS–PZT) is an ideal candidate for high-power applications in piezoelectric transformers, ultrasonic motors, and electromechanical transducers due to its superior electromechanical coupling factor, large mechanical quality factor and simultaneously low dissipation factor [1,2]. In these applications, high vibration velocities are usually desirable, implying that piezoelectric materials with low loss are expected to meet the demands of delivering high power [3]. It is well known that Mn is an effective acceptor dopant (hardening substitution) which can significantly stabilize the domain walls and thus enhance the mechanical quality factor Q_m, very promising for the high-power applications [4,5]. The hardening effect is frequently attributed to the aging process which is correlated with the gradual aligning of defect dipoles into the polarization direction [6–8]. Consequently, after fully aging, displaced or constricted polarization–electric field (*P–E*) loops can be observed in poled and unpoled hard piezoelectric ceramics [5,9–11].

Various stabilization mechanisms such as the grain boundary theory, domain wall theory, and volume theory have been proposed to explain these aging characteristics [9,12]. All these models can explain the aging phenomena to some extent while a general microscopic mechanism is still lacking. Recently, it has been verified that the domain stabilization is a defect dipole-related volume effect [13,14]. The constricted hysteresis loops are considered to be related with the pinning effect of defect dipoles, which are formed by acceptor ions and oxygen vacancies [7,9,10,13,14]. While the displaced *P–E* loops with internal bias field in poled ceramics can be attributed to the fact that the defect dipoles reorient to the poling direction by the diffusion of oxygen vacancies during the long-term aging [7,15]. The shift of the hysteresis curve along the *E*-axis

*Corresponding author. Tel.: +86 21 69906100; fax: +86 21 69906101.
E-mail address: xldong@sunm.shcnc.ac.cn (X. Dong).

0272-8842/$ - see front matter
http://dx.doi.org/10.1016/j.ceramint.2013.03.023

prevents the material from being switched or depolarized by moderate electric field. Therefore this effect is sometimes called stabilization effect [12,16,17]. On the other hand, it is well known that the defect dipoles are very sensitive to the operating conditions [18,19]. A cyclic bipolar electric field or a high temperature can cause the reorientation of the defect dipoles and thus induce the ferroelectric domain depinning process [18,19]. The pinning and depinning processes concerning the constricted *P–E* loops in unpoled piezoelectric ceramics have been extensively investigated in recent years [18–20]. However, the domain depinning properties with regard to the displaced *P–E* loops in poled ceramics are rarely studied. Actually, most of the piezoelectric ceramics in practical applications are poled and aged. It is thus crucial to directly characterize the relaxation processes of the displaced *P–E* loops in poled and aged ceramics for both high-power applications and theoretical analysis of domain dynamics.

In this work, temperature and electric field dependences of *P–E* and *S–E* loops in poled Mn-doped $Pb(Mn_{1/3}Sb_{2/3})O_3$–$Pb(Zr,Ti)O_3$ ceramics with internal bias field were systematically investigated. The relaxation (depinning) process of internal bias field was explained in terms of defect dipoles reorientation and domain wall motion.

2. Experimental procedure

The 0.1 wt% MnO_2 doped $0.05Pb(Mn_{1/3}Sb_{2/3})O_3$–0.50-$PbZrO_3$–$0.45PbTiO_3$ (abbreviated as Mn-doped PMS–PZT) ceramics were synthesized by conventional mixed oxide sintering route. Reagent-grade Pb_3O_4, $MnCO_3$, Sb_2O_3, ZrO_2, TiO_2, and MnO_2 (dopant) powders were mixed and ball-milled in ethanol for 6 h. After drying, the mixture was calcined at 850 °C for 2 h. Then the powder was re-milled and pressed into pellets of 10 mm in diameter and 1 mm in thickness using polyvinyl acetate (PVA) as adhesive. The pellets were sintered in a sealed alumina crucible at 1280 °C for 2 h under a PbO-rich atmosphere to minimize the lead loss during sintering. The sintered pellets were machined to 0.5 mm thickness and coated with silver electrodes on both sides. The samples were poled at 160 °C in a silicon oil bath under a DC field of 5 kV/mm for 15 min and then aged at room temperature for more than 1 month. The Curie temperature (T_C) of this ceramic determined from dielectric measurement was 566 K. Strain and polarization measurements were performed simultaneously using an aixACT TF 1000 analyzer (aixACT Systems GmbH, Aachen, Germany) equipped with a laser interferometer. The electric cycling experiment was conducted with a bipolar triangular electric signal with amplitude of 20 kV/cm at 20 Hz up to 10^5 cycles.

3. Results and discussion

Fig. 1 shows a comparison in the hysteresis (*P–E*) loop and electrostrain (*S–E*) curve for unaged and aged Mn-doped PMS–PZT ceramics after poling. It is noted that both samples exhibit an interesting displaced *P–E* loop similar to that of the accepter-doped PZT ceramics after poling and aging (Fig. 1(a)) [15]. Aging results in a slight increase in the coercive field and a significant increase in the extent of asymmetry in polarization and strain behaviors. However, the polarization is not affected by the aging process. Accompanying the asymmetric *P–E* loop, a large strain level of 0.60% at 30 kV/cm is achieved in the aged sample. This much larger change in the strain of the *S–E* loop with aging can be ascribed to the extrinsic domain switching contribution. As reported earlier, large domains (~10 μm) with smooth boundaries were found in the < 001 > textured $(K_{0.5}Na_{0.5})Nb_{0.97}Sb_{0.03}O_3$ ceramics in the aged condition due to the more readily redistribution of uniform and finer domain structures after poling [21]. This may be the case for our aged ceramics. The enhanced strain is believed to be related with the significant change in the domain distribution during aging. On the other hand, it has been reported that the internal bias field and the applied positive DC bias have the same effect on domain dynamics [22]. Therefore, the large strain in the right wing of the *S–E* loop for the aged Mn-doped PMS–PZT ceramic is attributed to the larger internal bias field which corresponds to a stronger interaction between defect dipoles and spontaneous polarization inside the domains. Further explanation can be found in the following part.

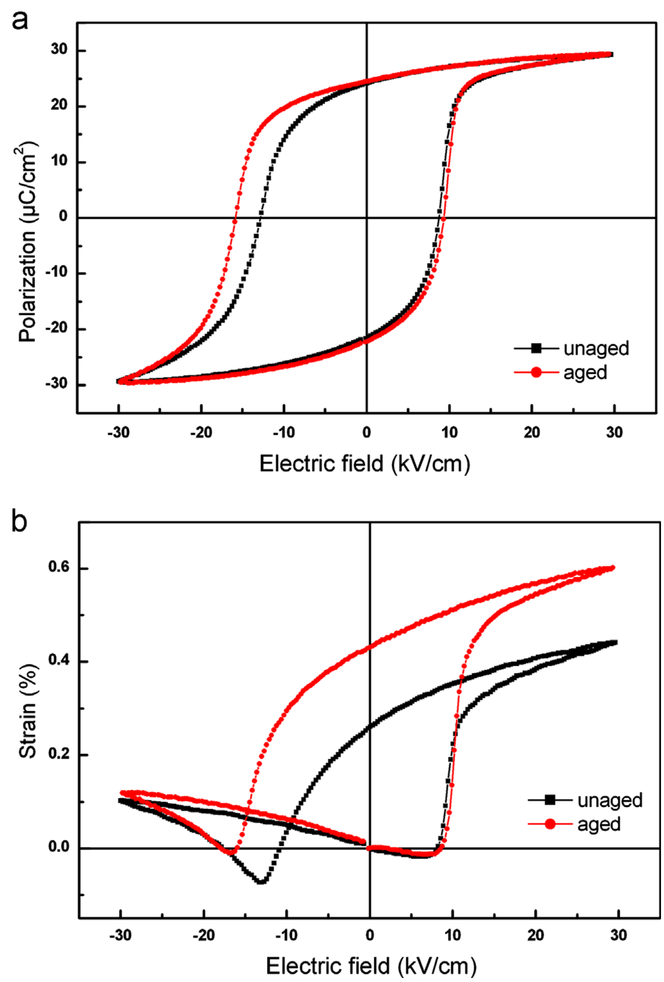

Fig. 1. (a) *P–E* hysteresis loops, and (b) *S–E* loops for unaged and aged Mn-doped PMS–PZT ceramics after poling.

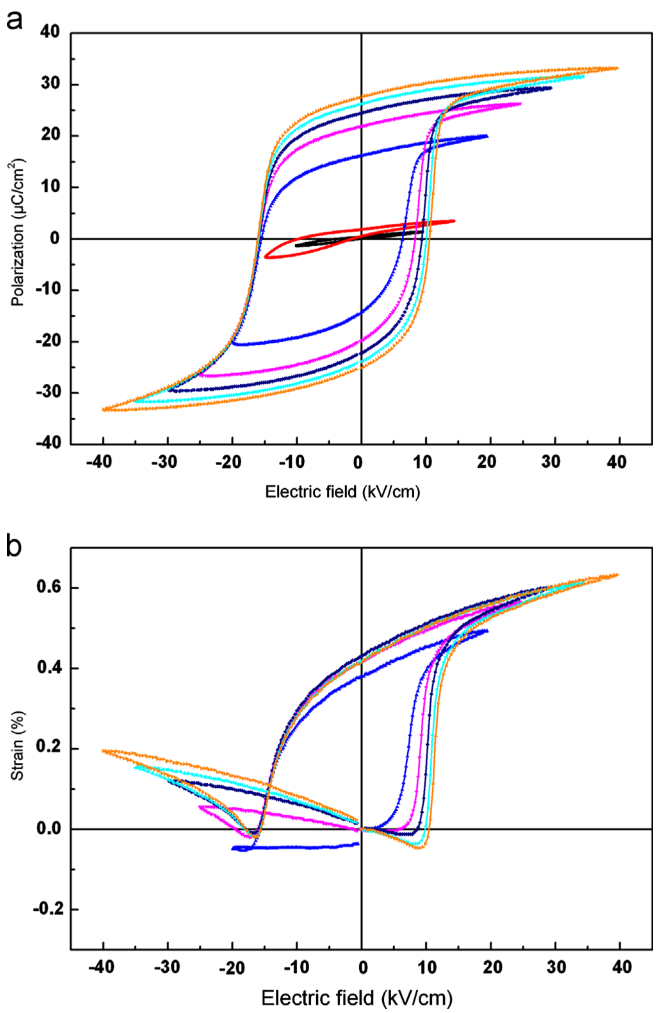

Fig. 2. (a) *P–E* hysteresis loops, and (b) *S–E* loops of Mn-doped PMS–PZT ceramics measured at 1 Hz as a function of applied electric field.

Fig. 2 shows the hysteresis loops of polarization *P*, strain *S* of aged Mn-doped PMS–PZT ceramics measured at 1 Hz as a function of applied electric field. It is noted that the *P–E* and *S–E* loops are strongly asymmetric, which indicate the presence of an internal bias field E_i. The magnitude of the E_i and the coercive field E_c can be determined by

$$E_i = \frac{E_+ + E_-}{2}, \quad E_c = \frac{E_+ - E_-}{2} \tag{1}$$

where E_+ and E_- are the intersections of polarization loops with positive and negative field axis, respectively [9]. To date, three mechanisms have been proposed to describe the defect-induced stabilization of domain structure in acceptor doped ferroelectric materials. They differ in the location of the defects that stabilize the domain configuration: within domains (the volume effect), in the domain wall region (the domain wall effect), and on the grain boundaries (the grain boundary effect) [12]. Among these mechanisms, the defect dipoles related volume effect is dominated and has been experimentally confirmed in aged $BaTiO_3$ single crystals by Ren [14]. In the following, we will focus our discussion on defect dipoles as the most probable origin of the asymmetric hysteresis loops. It has been suggested that Mn^{4+} occupies the B-site of perovskite structure and will be reduced to Mn^{2+} and Mn^{3+} during sintering, which leads to the formation of oxygen vacancies ($V_O^{\bullet\bullet}$) to keep electrical neutrality [4,23,24]. Based on the symmetry-conforming principle of point defects [14,25,26], during DC poling at 160 °C, the defects migrate easily and the defect dipoles are formed by the acceptor dopant ions (Mn^{2+}/Mn^{3+}) and O^{2-} vacancies along the direction of aligned polarization, creating an internal bias field and stabilizing the domain configuration. As a result, the ceramic is hardened, giving a large Q_m~500 after aging. Whereas, with increasing electric field, the shape of the *P–E* loops exhibits a tendency of changing from asymmetric loops to square ones and the E_i reduces gradually from 4.62 kV/cm at 20 kV/cm to 2.86 kV/cm at 40 kV/cm, which may be caused by the partial realignment of oxygen vacancies under higher driving electric field. That is to say, some of the pinning sites decouple from the domain boundaries and the defect dipoles relax under higher electric field. On the other hand, notably asymmetric *S–E* loops in respect to the electric field axis are observed in the poled Mn-doped PMS–PZT ceramics, as shown in Fig. 2(b). It should be noted that there are two stable states of the strain hysteresis at zero electric field. And this is different from the single stable state for conventional symmetric *S–E* loops at zero electric field, which suggests that a strain memory effect can be induced in poled hard piezoelectrics. Novel piezoelectric actuators, which could keep its output strain without any operating fields, may be fabricated using this kind of material.

The frequency dependence of the *P–E*, *S–E* loops for the Mn-doped PMS–PZT ceramics was investigated in the range of 0.01–10 Hz, and the results are shown in Fig. 3. It can be seen that the remnant polarization P_r increases and the E_i decreases with decreasing frequency. In the high frequency measurements, the polarization is switched abruptly by the external field, while the defect dipoles remain in the original direction due to insufficient time for the oxygen vacancies to migrate [27]. However, when the frequency is lowered, some of the vacancies may have enough time to migrate and thus the domain walls are depinned to some extent. Accordingly, the pinning effect decreases and domain switching becomes easier, giving larger P_r. It should be noticed that the internal bias field was rather stable in comparison with PMnN–PZT ceramics, in which it was found that the E_i decreased to zero with frequency decreasing down to 0.01 Hz [19].

It is reported that the electric field cycling can depin the domain walls and improve the remnant polarization [9,18]. Fig. 4 shows the *P–E*, *S–E* loops obtained in an aged sample and after applying various electric cycles. Displaced *P–E* loop and asymmetric *S–E* loop are clearly observed in the aged state in agreement with the previous results for the poled and aged hard ferroelectrics [9,15]. However, the distortion of the asymmetric loops is alleviated to some extent with increasing the cycling numbers. The right wing of the strain curve decreases and the symmetry of the *S–E* loop increases during the cycling process (Fig. 4(b)). The internal bias field is not completely relaxed even after 10^5 cycles. Fig. 5 quantifies the changes of the switchable polarization ($2P_r$) and the E_i as a function of the electric field cycles. During the cycling, the

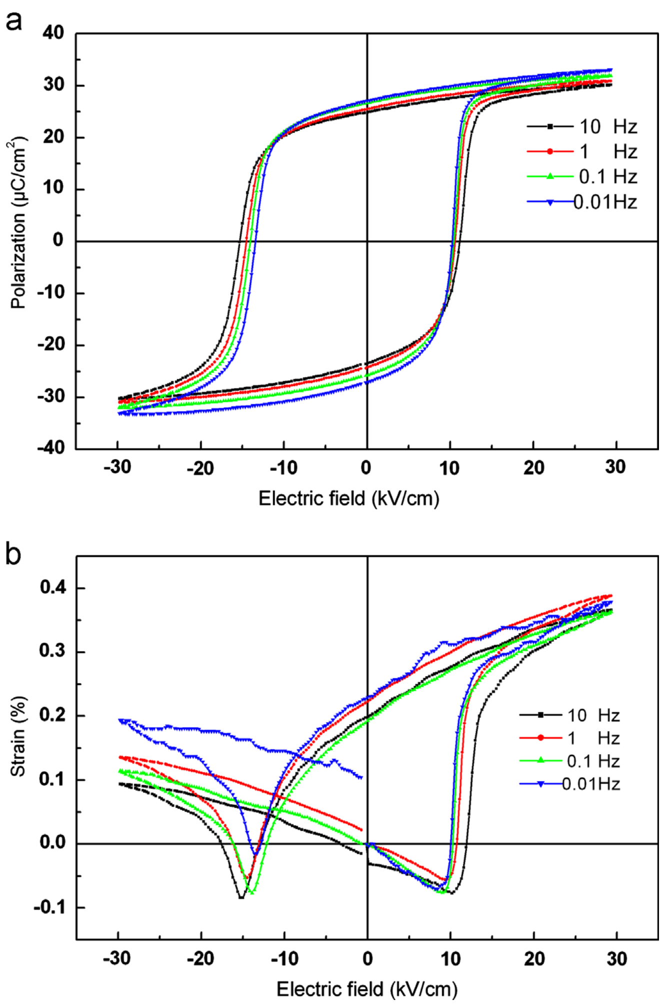

Fig. 3. Frequency dependence of the (a) *P–E* hysteresis loops, and (b) *S–E* loops for Mn-doped PMS–PZT ceramics.

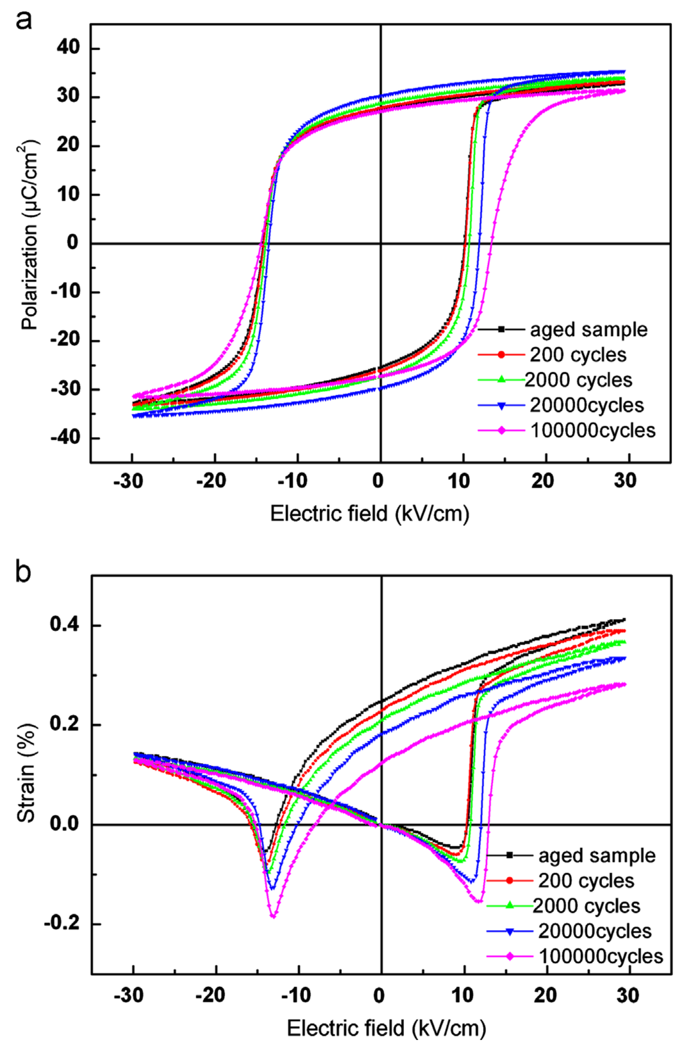

Fig. 4. (a) *P–E* hysteresis loops, and (b) *S–E* loops obtained in an aged sample and after applying various electric cycles for Mn-doped PMS–PZT ceramics.

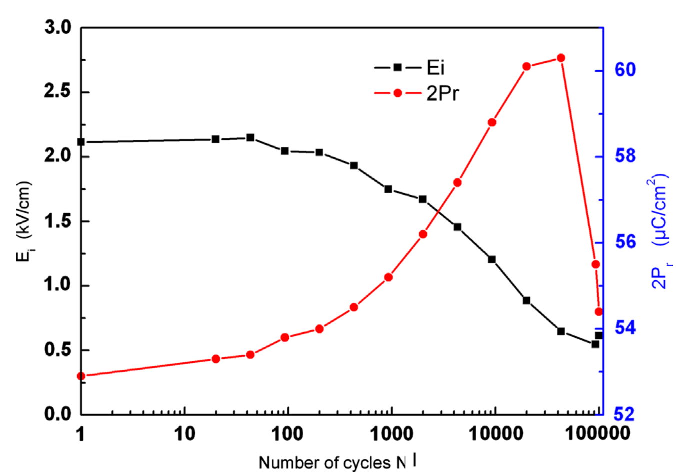

Fig. 5. Switchable polarization ($2P_r$) and internal bias field (E_i) as a function of the number of cycles.

ceramic exhibits a maximum in $2P_r$ after about 4×10^4 cycles. The increase in $2P_r$ can be explained by an initial domain wall depinning, while the subsequent decrease can be attributed to a fatigue process, which has also been observed in various ferroelectric ceramics [16]. Whereas, the E_i decreases significantly up to 9×10^4 cycles and then shows an increasing tendency during the fatigue process, as depicted in Fig. 5.

Since the samples are aged in the poled state, it is expected that the domain walls are clamped by defect dipoles which align in the direction of spontaneous polarization within the individual domains [7,14]. As mentioned in the previous literatures [9,14], the defect dipole realignment mostly occurs locally through the hopping of oxygen vacancies. Application of a cycling bipolar electric field is supposed to redistribute the oxygen vacancies or reorient the defect dipoles and thus reduce the clamping effect on the domain walls, which may contribute to the increase of switchable polarization. As a result, the E_i relaxes progressively during the cycling. It should be noted that the ferroelectric loops of these samples do not become symmetrical with field cycling, suggesting a strong domain wall pinning effect differs from the totally depinned loops observed after 500 cycles in 0.8 at% Fe-doped $Pb(Zr0_{.58}Ti_{0.42})O_3$ ceramics [9]. After about 4×10^4 cycles, the switchable polarization degrades from 60.3 $\mu C/cm^2$ to 54.4 $\mu C/cm^2$, indicating a fatigue process which may be ascribed to the

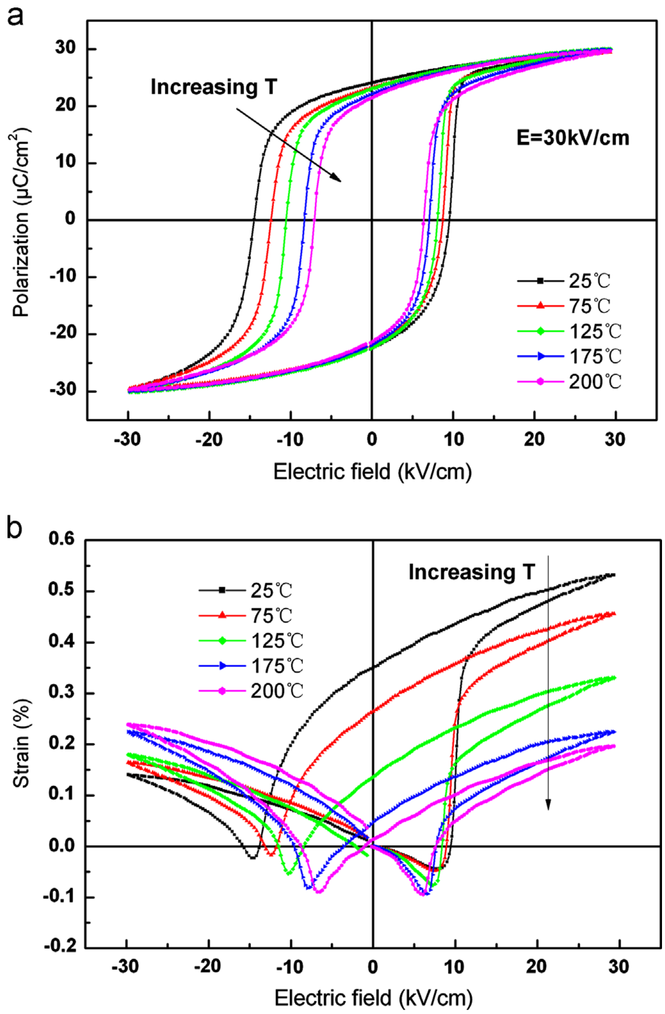

Fig. 6. Temperature dependence of (a) *P–E* hysteresis loops, and (b) *S–E* loops measured at $E=30$ kV/cm for Mn-doped PMS–PZT ceramics.

domain wall stabilization or the presence of microstructural damage during bipolar fatigue [28].

To provide additional evidence for the internal bias field relaxation, the temperature dependence of the *P–E*, *S–E* responses of this Mn-doped PMS–PZT ceramics was performed from 25 °C to 200 °C, and the results are shown in Fig. 6. The evolution of *P–E* or *S–E* loop with increasing temperature is similar to that of increasing the cycling number or decreasing the frequency. With increasing temperature, the hysteresis loops gradually become symmetric and nearly normal *P–E* loop and butterfly strain curve can be obtained when the temperature reaches 200 °C. Interestingly, the P_r and the maximum polarization P_{max} are rather stable with temperature, which is believed to be related to the defect dipoles and the correspondingly internal bias field [29]. Fig. 7 summarizes the internal bias field E_i and the loop area $<A>$ as a function of temperature for $E=30$ kV/cm. The E_i decreases significantly from 2.76 kV/cm to 0.43 kV/cm when the temperature increases from room temperature to 200 °C. The overall changing tendency in the loop area $<A>$ follows a similar manner as the E_i.

As stated above, the defect symmetry in each domain follows the polar crystal symmetry after aging. The

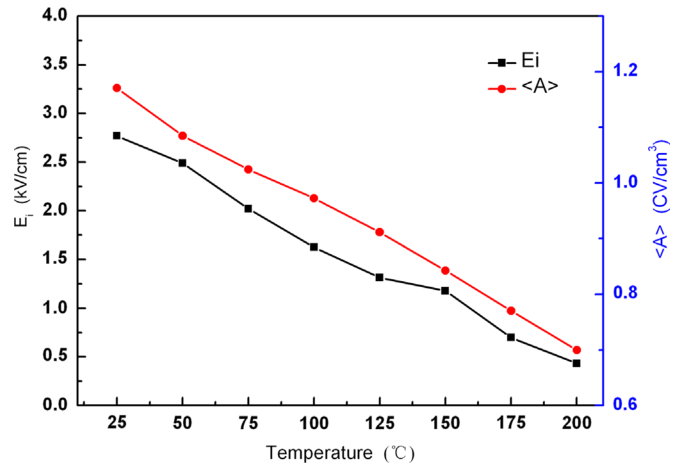

Fig. 7. Internal bias field (E_i) and hysteresis loop area $<A>$ as a function of temperature for $E=30$ kV/cm.

configuration of (Mn^{2+}/Mn^{3+}) dopant and $V_O^{\bullet\bullet}$ exhibits a defect dipole moment P_D following the spontaneous polarization P_S direction, forming an internal bias field that stabilizes the domains and results in "hard" characteristics [14]. Nevertheless, at high temperature, the mobility of the vacancies or the defect dipoles increases, and therefore the reorientation of the defect dipoles can follow the electric field change. That is, the disordering of the pinning centers results in the randomization of the energy profile for domain walls. Hence, the thermal energy of the domains decreases and lower activation energy is required to make domain switching. In addition, it is reported that the lattice distortion reduces at elevated temperature which further facilitates the domain switching [30]. All these changes are responsible for the continuous decrease of E_i and E_c, and accordingly the hysteresis loops gradually become symmetric and nearly normal *P–E*, *S–E* loops are obtained with slight internal bias field at 200 °C.

4. Conclusion

The *P–E*, *S–E* loops of the poled Mn-doped $0.05Pb(Mn_{1/3}Sb_{2/3})O_3$–$0.50PbZrO_3$–$0.45PbTiO_3$ ceramics are asymmetric along the *E*-axis at room temperature, which may be attributed to the formation of internal bias field along the poling direction. Based on the symmetry-conforming principle of point defects, the internal bias field can be explained by the interaction between the spontaneous polarization and the defect dipoles composed of the acceptor dopant ions (Mn^{2+}/Mn^{3+}) and O^{2-} vacancies, and the domain wall mobility is reduced due to the ordered defects. However, the internal bias E_i and coercive field E_c are significantly affected by the temperature and the applied electric field. At high temperature or after applying various electric field cycles, the mobility of the vacancies or the defect dipoles increases and the disordering of the pinning centers results in the fact that the reorientation of the defect dipoles can follow the electric field change. Thus, E_i relaxed gradually under these conditions.

Acknowledgments

This work was supported by Chinese Academy of Sciences Research Equipment Development Project (Grant no.YZ201141).

References

[1] Z.G. Zhu, G.R. Li, Z.J. Xu, W.Z. Zhang, Q.R. Yin, Effect of PMS modification on dielectric and piezoelectric properties in xPMS–$(1-x)$PZT ceramics, Journal of Physics D: Applied Physics 38 (2005) 1464–1469.

[2] H. Du, S. Qu, J. Che, Z. Liu, X. Wei, Z. Pei, The effect of composition on microstructure and properties of PNW–PMS–PZT ceramics for high-power piezoelectric transformer, Materials Science and Engineering A 393 (2005) 36–41.

[3] Z.G. Zhu, G.R. Li, B.S. Li, Q.R. Yin, K.L. Jiang, The influence of Yb and Nd substituents on high-power piezoelectric properties of PMS–PZT ceramics, Ceramics International 34 (2008) 2067–2072.

[4] L.X. He, C.E. Li, Effects of addition of MnO on piezoelectric properties of lead zirconate titanate, Journal of Materials Science 35 (2000) 2477–2480.

[5] S. Takahashi, Effects of impurity doping in lead zirconate–titanate ceramics, Ferroelectrics 41 (1982) 143–156.

[6] L. Zhang, X. Ren, Aging behavior in single-domain Mn-doped $BaTiO_3$ crystals: implication for a unified microscopic explanation of ferroelectric aging, Physical Review B 73 (2006) 094121.

[7] U. Robels, G. Arlt, Domain wall clamping in ferroelectrics by orientation of defects, Journal of Applied Physics 73 (1993) 3454–3460.

[8] P. Jakes, E. Erdem, R.A. Eichel, L. Jin, D. Damjanovic, Position of defects with respect to domain walls in Fe^{3+}-doped $Pb[Zr_{0.52}Ti_{0.48}]O_3$ piezoelectric ceramics, Applied Physics Letters 98 (2011) 072907.

[9] K. Carl, K.H. Hardtl, Electrical after-effects in $Pb(Ti, Zr)O_3$ ceramics, Ferroelectrics 17 (1978) 473–486.

[10] Q. Tan, J. Li, D. Viehland, Role of lower valent substituent-oxygen vacancy complexes in polarization pinning in potassium-modified lead zirconate titanate, Applied Physics Letters 75 (1999) 418–420.

[11] D. Damjanovic, Ferroelectric,dielectric and piezoelectric properties of ferroelectric thin films and ceramics, Reports on Progress in Physics 61 (1998) 1267–1324.

[12] P. Lambeck, G. Jonker, The nature of domain stabilization in ferroelectric perovskites, Journal of Physics and Chemistry of Solids 47 (1986) 453–461.

[13] Z. Feng, O. Tan, W. Zhu, Y. Jia, H. Luo, Aging-induced giant recoverable electrostrain in Fe-doped 0.62 Pb $(Mg_{1/3}Nb_{2/3})$ O_3–0.38 $PbTiO_3$ single crystals, Applied Physics Letters 92 (2008) 142910.

[14] X.B. Ren, Large electric-field-induced strain in ferroelectric crystals by point-defect-mediated reversible domain switching, Nature Materials 3 (2004) 91–94.

[15] T.M. Kamel, Poling of hard ferroelectric PZT ceramics, Journal of the European Ceramic Society 28 (2008) 1827–1838.

[16] T. Rojac, M. Kosec, B. Budic, N. Setter, D. Damjanovic, Strong ferroelectric domain-wall pinning in $BiFeO_3$ ceramics, Journal of Applied Physics 108 (2010) 074107.

[17] Z.-Y. Shen, Y. Xu, J.-F. Li, Enhancement of Q_m in CuO-doped compositionally optimized Li/Ta-modified $(Na,K)NbO_3$ lead-free piezoceramics, Ceramics International 38 (Suppl. 1) (2012) S331–S334.

[18] Y. Gao, K. Uchino, D. Viehland, Domain wall release in "hard" piezoelectric under continuous large amplitude ac excitation, Journal of Applied Physics 101 (2007) 114110.

[19] B.S. Li, G.R. Li, Q.R. Yin, Z.G. Zhu, A.L. Ding, W.W. Cao, Pinning and depinning mechanism of defect dipoles in PMnN–PZT ceramics, Journal of Physics D: Applied Physics 38 (2005) 1107–1111.

[20] Q. Tan, Z. Xu, J.F. Li, D. Viehland, Role of defect distributions and mobility on ferroelectric phase transformations in lead zirconate titanate, Applied Physics Letters 71 (1997) 1062–1064.

[21] J. Yao, J. Li, D. Viehland, Y. Chang, G.L. Messing, Aging associated domain evolution in the orthorhombic phase of $<001>$ textured $(K_{0.5}Na_{0.5})Nb_{0.97}Sb_{0.03}O_3$ ceramics, Applied Physics Letters 100 (2012) 132902.

[22] Y. Gao, K. Uchino, D. Viehland, Effects of thermal and electrical histories on hard piezoelectrics: a comparison of internal dipolar fields and external dc bias, Journal of Applied Physics 101 (2007) 054109.

[23] Y. Hou, M. Zhu, F. Gao, H. Wang, B. Wang, H. Yan, C. Tian, Effect of MnO_2 addition on the structure and electrical properties of $Pb(Zn_{1/3}Nb_{2/3})_{0.20}$ $(Zr_{0.50}Ti_{0.50})_{0.80}O_3$ ceramics, Journal of the American Ceramic Society 87 (2004) 847–850.

[24] E. Boucher, B. Guiffard, L. Lebrun, D. Guyomar, Effects of Zr/Ti ratio on structural, dielectric and piezoelectric properties of Mn- and (Mn, F)-doped lead zirconate titanate ceramics, Ceramics International 32 (2006) 479–485.

[25] D. Lin, K. Kwok, H. Chan, Double hysteresis loop in Cu-doped $K_{0.5}Na_{0.5}NbO_3$ lead-free piezoelectric ceramics, Applied Physics Letters 90 (2007) 232903.

[26] Z. Feng, X. Ren, Aging effect and large recoverable electrostrain in Mn-doped $KNbO_3$-based ferroelectrics, Applied Physics Letters 91 (2007) 032904.

[27] M.H. Lente, A. Picinin, J.P. Rino, J.A. Eiras, 90° domain wall relaxation and frequency dependence of the coercive field in the ferroelectric switching process, Journal of Applied Physics 95 (2004) 2646–2653.

[28] N. Balke, D.C. Lupascu, T. Granzow, J. Rödel, Fatigue of lead zirconate titanate ceramics I: unipolar and DC loading, Journal of the American Ceramic Society 90 (2007) 1081–1087.

[29] R. Yimnirun, A. Ngamjarurojana, R. Wongmaneerung, S. Wongsaenmai, S. Ananta, Y. Laosiritaworn, Temperature scaling of ferroelectric hysteresis in hard lead zirconate titanate bulk ceramic, Applied Physics A 89 (2007) 737–741.

[30] F. Li, Z. Xu, X.Y. Wei, X. Yao, Temperature- and dc bias field-dependent piezoelectric effect of soft and hard lead zirconate titanate ceramics, Journal of Electroceramics 24 (2010) 294–299.